

Enhanced Coupling of Electron and Nuclear Spins by Quantum Tunneling Resonances

Anatoli Tsinovoy^{1,2}, Or Katz^{2,*}, Arie Landau^{3,4} and Nimrod Moiseyev^{1,4}

¹Faculty of Physics, Solid State Institute, Technion-Israel Institute of Technology, Haifa 3200003, Israel

²Rafael, Ltd., Haifa 3102102, Israel

³Institute of Advanced Studies in Theoretical Chemistry, Technion-Israel Institute of Technology, Haifa 3200003, Israel

⁴Schulich Faculty of Chemistry, Technion-Israel Institute of Technology, Haifa 3200003, Israel

Ⓞ (Received 20 October 2020; revised 10 September 2021; accepted 29 November 2021; published 4 January 2022)

Noble-gas spins feature hours-long coherence times, owing to their great isolation from the environment, and find practical usage in various applications. However, this isolation leads to extremely slow preparation times, relying on weak spin transfer from an electron-spin ensemble. Here we propose a controllable mechanism to enhance this transfer rate. We analyze the spin dynamics of helium-3 atoms with hot, optically excited potassium atoms and reveal the formation of quasibound states in resonant binary collisions. We find a resonant enhancement of the spin-exchange cross section by up to 6 orders of magnitude and 2 orders of magnitude enhancement for the thermally averaged, polarization rate coefficient. We further examine the effect for various other noble gases and find that the enhancement is universal. We outline feasible conditions under which the enhancement may be experimentally observed and practically utilized.

DOI: [10.1103/PhysRevLett.128.013401](https://doi.org/10.1103/PhysRevLett.128.013401)

Spin-polarized noble gases are unique systems that can maintain their spin state for hours, even at room temperature. They have utility in various applications, including precision sensing [1–4], medical imaging of the brain and lungs [5–9], neutron scattering experiments [10,11], the search for dark matter, physics beyond the standard model [12–15], and potentially in quantum information applications, including the generation of long-lived entanglement [16–20].

The great isolation of noble-gas spins from the environment sets a trade-off between their spin-polarization rate and their spin lifetime. The primary polarization processes for noble-gas spins rely on spin changing collisions with other atoms whose spins can be optically manipulated, such as metastable excited noble gases [21–27] or alkali vapor in the ground state [28–32]. While both processes are practically useful, the former approach is mostly useful for helium and relies on electrical discharge, which constantly generates plasma. The plasma limits both spin lifetime and the fraction of optically accessible atoms [10], thus narrowing the applicability and hindering miniaturization of this approach.

Collisions with alkali atoms benefit from higher possible densities and longer spin lifetimes. It can be applied to all noble gases and miniaturized to a greater extent [2]. Here, the polarization rate is determined by collisions of alkali and noble-gas pairs, illustrated in Fig. 1. While heavy noble gases can be polarized quickly, their spin lifetime is considerably shorter than light noble gases. ³He, in particular, exhibits the longest spin lifetime but also the weakest coupling to alkali spins, rendering its polarization

rate extremely slow. At typical conditions, ³He polarization takes many tens of hours, limiting its utility.

In cold atomic and molecular gases, interaction during collisions can be greatly enhanced by quantum Feshbach or tunneling resonances [33–43]. Tunneling resonances prolong the interaction time via the formation of quasibound states at particular values of the kinetic energy. At room temperature and above, however, the collision dynamics comprise many tens of partial waves, the atoms follow a thermal energy distribution, and measured cross sections

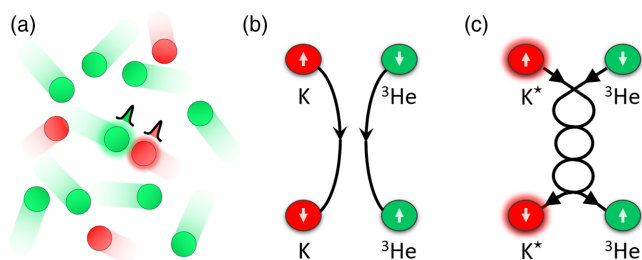


FIG. 1. Enhancement of spin-polarization rate via quantum tunneling resonances. (a) Alkali atoms and noble-gas atoms experience frequent spin-exchange collisions. At room temperature, the quantum nature of atomic motion, such as tunneling resonances, is obscured. (b) Spin exchange in a short binary collision between a ground-state alkali atom and a noble-gas atom. The probability of spin exchange per collision is extremely small, resulting in slow spin-polarization rate. (c) Resonant spin exchange between an electronically excited alkali atom and a noble-gas atom. In resonant collisions, a quasibound state is formed and interaction time is increased by orders of magnitude, significantly enhancing the probability of spin exchange.

attain their classically predicted values [31,44]. It is therefore generally assumed that quantum resonances at ambient conditions would be negligible, and consequently, their potential application for noble-gas polarization has never been considered.

Here we propose a new mechanism to enhance the polarization rate of noble-gas spins by resonant collisions with electronically excited alkali atoms. We solve the quantum scattering problem of ^3He colliding with electronically excited potassium and reveal tunneling resonances in binary collisions [45–48]. We calculate the spin-polarization rate coefficient and find 2 orders of magnitude enhancement driven by the resonances and up to 6 orders of magnitude enhancement of the spin-exchange cross section at specific resonance energies. We analyze the application of this mechanism to other alkali and noble-gas pairs and find universal enhancement. Finally, we outline the conditions under which the enhancement may be experimentally observed and practically utilized.

We start the analysis by solving the quantum scattering of alkali and noble-gas pairs. We then consider the energy-dependent elastic and spin-exchange cross sections and finally calculate the thermally averaged rate coefficient of the ensemble.

We describe the motion of the pair during a collision using the Born-Oppenheimer approximation, separating the nuclear and electronic degrees of freedom. The Hamiltonian for the relative motion of the nuclei is given by

$$H = -\frac{\hbar^2}{2\mu} \frac{\partial^2}{\partial R^2} + \frac{\hbar^2 \mathbf{L}^2}{2\mu R^2} + V(R) + \hbar\alpha(R) \mathbf{I} \cdot \mathbf{S}. \quad (1)$$

The first two terms describe the kinetic energy, where R denotes the internuclear distance, \mathbf{L}^2 denotes the rotational angular momentum of the relative motion of the nuclei with eigenvalues $l(l+1)$, and μ denotes the reduced mass of the pair. The third term $V(R)$ describes the spin-independent potential energy curve (PEC), and the last term is the spin-dependent interaction, dominated by the isotropic Fermi contact term [32]. This interaction is responsible for the spin-polarization transfer from the electronic spin of the potassium atom \mathbf{S} to the nuclear spin of the helium \mathbf{I} via the hyperfine-coupling coefficient $\alpha(R)$.

We calculate the *ab initio* values of $V(R)$ and $\alpha(R)$ for the $\text{K-}^3\text{He}$ complex as shown in Fig. 2(a) for the $X^2\Sigma(4S)$ ground state and $^2\Sigma$ excited states. The wave functions of the isolated K atom and the $\text{K-}^3\text{He}$ complex are constructed hierarchically. First we solve the restricted Hartree Fock equations for the $(\text{K-}^3\text{He})^+$ cation (a closed shell system that serves as a reference function). We then refine the results by introducing correlations using the equation-of-motion coupled-clusters method at the singles and doubles level of theory. Finally, the valence electron is added via electron attachment [49,50]. The calculations are performed via the electronic-structure package Q-CHEM [51],

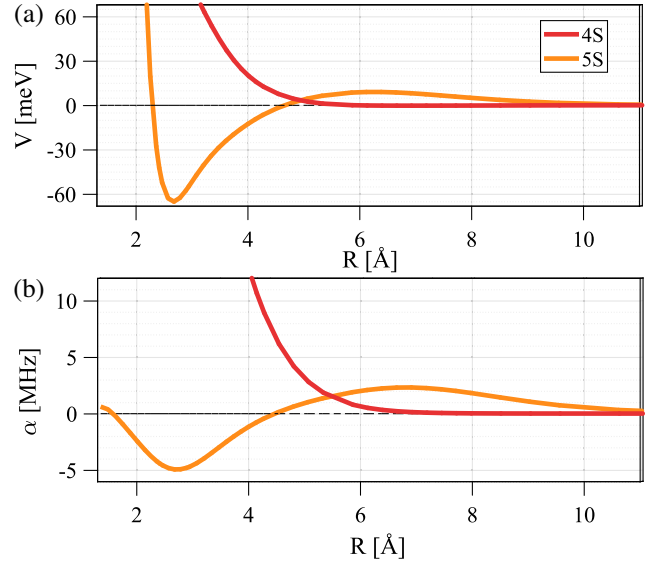


FIG. 2. Potential energy curves and hyperfine-coupling coefficient for helium-3 and electronically excited potassium. (a) PEC of the $\text{K-}^3\text{He}$ complex, corresponding asymptotically to the helium atom in its ground state and to the potassium atom in its $4S$ ground state or its $5S$ electronically excited state. The ground-state potential (red) is purely repulsive, whereas the excited state (orange) exhibits a potential well and a barrier. (b) Hyperfine-coupling coefficient $\alpha(R)$. The sign of $\alpha(R)$ simply indicates the precession direction of the spins.

with $V(R)$ and the electronic wave function $|\Psi(R)\rangle$ as outputs, where the latter is used to calculate $\alpha(R)$ directly [32,52]. Comparison with Ref. [53] for validation and the results for the first dozen excited states are provided in the Supplemental Material [54].

For collisions of helium and potassium in the ground state, the $X^2\Sigma(4S)$ potential is purely repulsive and supports no bound or quasibound states. In contrast, the excited-state $^2\Sigma(5S)$ potential exhibits a potential well preceded by a barrier. The barrier is significant even for s -wave collisions ($l=0$), in the absence of a centrifugal potential. These wells and barriers give rise to bound states ($E < 0$) and quasibound states [45,46] ($E > 0$) as shown in Fig. 3(a). The wave functions of both the bound and quasibound states (square-integrable rovibrational solutions) were obtained by the method of complex scaling [45] and are presented superimposed on the PEC.

To quantify the contribution of the quasibound states to the polarization rate, we solve the quantum scattering problem via the method of Siegert pseudostates [67], which is suitable for single-channel problems. We exploit the symmetry of $\hbar\alpha(R) \mathbf{I} \cdot \mathbf{S}$ in Eq. (1), which is diagonal with respect to the joint angular momentum operator $\mathbf{J}^2 \equiv (\mathbf{I} + \mathbf{S})^2$ with eigenvalues $j(j+1)$, and solve the scattering of the singlet and triplet channels independently.

For each single-channel problem, we use $N = 200$ basis functions (Jacobi polynomials [68]) to discretize the

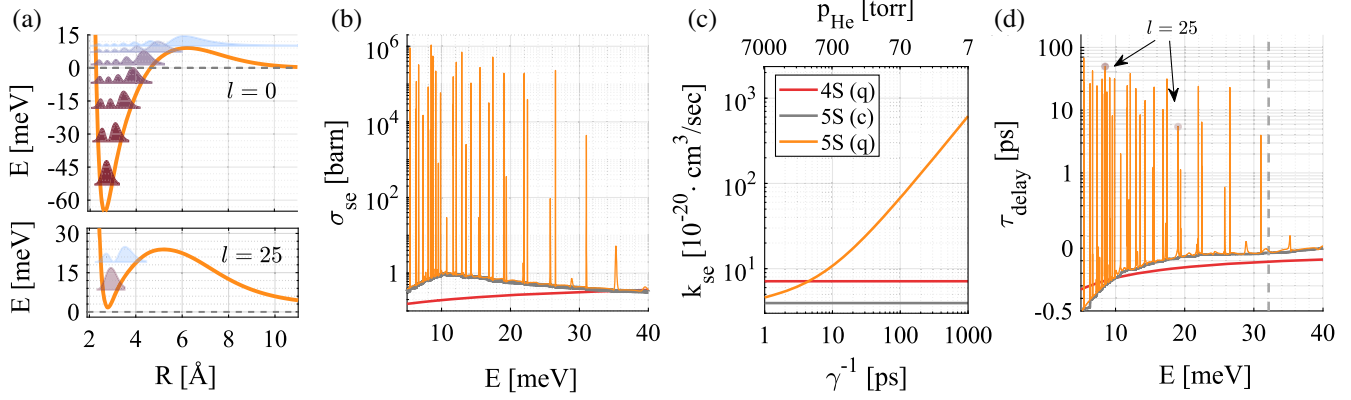


FIG. 3. Tunneling resonances in binary collisions. (a) PEC for the $5S$ state with $l = 0$ (top) and $l = 25$ (bottom), superimposed with the wave function of bound states ($E < 0$) and quasibound states ($E > 0$) at their resonance energies. (b) The spin-exchange cross section $\sigma_{\text{se}}^{(q)}(E)$ of the $5S$ state (orange) is dramatically enhanced at the resonances, by up to 6 orders of magnitude with respect to that cross section absent the resonances, $\sigma_{\text{se}}^{(c)}(E)$ (gray). (c) Thermally averaged polarization rate coefficient $k_{\text{se}}^{(q)}$ at 100°C . $k_{\text{se}}^{(q)}$ for collisions of ${}^3\text{He}$ with K^* in the $5S$ state (orange) is enhanced by up to 2 orders of magnitude by the resonances at low pressures. (d) Scattering time delay, relative to a hard-wall potential at the origin, for a binary collision at energy E and $j = 0$. Sharp peak resonances signify the formation of quasibound states, enhancing the typical duration of semiclassical binary collisions (0.1 ps) by 3 orders of magnitude. Vertical dashed lines in (d) mark the mean thermal energy at 100°C , and arrows exemplify the dominant resonant contribution of a specific partial wave $l = 25$ to the time delay. Gray lines in (b)–(d) present semiclassical estimations for the $5S$ state, which exclude the contribution of the resonances. The semiclassical limit is reached for high values of γ , where the resonances are suppressed and the collisions are entirely classical.

problem and construct a matrix representation of Eq. (1). We truncate the problem at $a = 40a_0$, explicitly approximating $V(R) \approx 0$ for $R > a$, having verified convergence. Diagonalization of this matrix yields a discrete set of complex wave numbers $k_{n,l,j}$ associated with all incoming and outgoing collision states, including the long-lived tunneling resonances. To account for shortening of the resonance lifetimes by other processes, we introduce a relaxation rate γ into the calculation by $\tilde{k}_{n,l,j} = \text{Re}(k_{n,l,j}) + i[\text{Im}(k_{n,l,j}) - \gamma/|k_{n,l,j}|]$, where γ describes the external dissociation rate. We model $\gamma = \gamma_0 + ap$ to account for spontaneous emission at a typical rate $\gamma_0^{-1} \approx 10$ ns and for collisions with background atoms at characteristic pressure p at room temperature. While the molecular dissociation rate of stable alkali-noble-gas molecules in the S manifold is about 1 MHz/Torr [69], here we consider a more stringent rate that bounds the dissociation rate of quasibound molecules due to collisions with a second helium atom. As the charge density of helium is strongly localized, perturbations to the resonance states can occur only when the second helium atom overlaps with the $\text{K}-{}^3\text{He}$ wave function, at most 5 \AA from its center, yielding $a \lesssim \sigma_{\text{hard sphere}} v = 25 \times 2\pi \text{ MHz/Torr}$. The partial scattering amplitudes are then given by [67]

$$S_l^j(E) = e^{-2i\sqrt{2E}a} \prod_{n=1}^{2N+l} \frac{\tilde{k}_{n,l,j} + \sqrt{2E}}{\tilde{k}_{n,l,j} - \sqrt{2E}}, \quad (2)$$

and the quantum spin-exchange cross section is given by the sum

$$\sigma_{\text{se}}^{(q)}(E) = \frac{\pi}{8E} \sum_l (2l+1) |S_l^1 - S_l^0|^2. \quad (3)$$

We present the spin-exchange cross section in Fig. 3(b) for collisions of ground- (red) or excited-state (orange) potassium with a lifetime limit of $\gamma^{-1} = 1$ ns corresponding to 7 Torr of ${}^3\text{He}$. The $5S$ state exhibits considerable increase at sharply defined peaks at specific resonant values of the kinetic energy. To highlight the role of these resonances, we first compare $\sigma_{\text{se}}^{(q)}$ with the semiclassical estimate of Ref. [70], as shown in Fig. 3(b) (gray) and given by

$$\sigma_{\text{se}}^{(c)}(E) = \frac{\pi}{2} \int_0^\infty b db \left| \int_{-\infty}^\infty \alpha(R(t)) dt \right|^2. \quad (4)$$

This estimate integrates the hyperfine interaction across all possible classical collision trajectories at energy E .

At specific energies, the ratio $\sigma_{\text{se}}^{(q)}/\sigma_{\text{se}}^{(c)}$ for the $5S$ state spans up to 6 orders of magnitude. At room temperature or above, however, the practical polarization rate is determined by the rate coefficient $k_{\text{se}}^{(q)}$, which averages the spin-exchange cross section over the Boltzmann distribution at temperature T . In Fig. 3(c), we present the polarization rate coefficient of the ground state (red) and excited state (orange) at 100°C as a function of the inverse external dissociation rate γ^{-1} . Evidently, for long-collision-lifetime limits, the excited-state polarization rate surpasses that of the ground state by up to 2 orders of magnitude. This

enhancement is due to quantum resonances, as seen by comparison with the semiclassical estimate (gray) of the rate coefficient $k_{se}^{(c)}$.

Before detailing the experimental proposal for measuring this enhancement and discussing its potential applications, we find it insightful to discuss its origin and its expected manifestation in other alkali and noble-gas pairs. As suggested by the semiclassical formula, Eq. (4), the cross section is determined by the interaction strength $|\alpha(R)|^2$, integrated over the duration of the collision. As shown in Fig. 2(b), $|\alpha(R)|$ is comparable for the ground and excited states, implying that the resonant enhancement is due to an increase in interaction time.

We estimate the interaction time by calculating the temporal delay (or acceleration) of a particle with energy E and angular momentum j scattered by $V(R)$, relative to its free-flight time. In Fig. 3(d) we present the mean time delay $\tau_{\text{delay}}^j(E) = \sum_l \sigma_l^j \tau_l^j / \sum_l \sigma_l^j$ for $\gamma^{-1} = 1$ ns. $\tau_l^j = 2d\delta_l^j/dE$ are the partial delays, $\sigma_l^j(E) = (8\pi/E)(2l+1)\sin^2\delta_l^j$ are the partial elastic cross sections, and $\delta_l^j(E) = -(i/2)\log S_l^j$ are the partial scattering phase shifts [71]. For K-³He in the 5S excited state, the time-delay features sharp peaks like those in Fig. 3(b), unlike the smooth ground-state response. These peaks are associated with tunneling resonances, where the mean time delay corresponds to the lifetime of the quasibound state. Notably, the width of a resonance is inversely proportional to its lifetime, but its contribution to the spin-exchange cross section scales as its lifetime squared. This allows a finite number of narrow resonances to dominate the polarization rate coefficient. We have repeated this analysis for other estimations of the PEC [72,73] and found that the enhancement of the rate coefficient remains considerable (see the Supplemental Material [54]).

We expect polarization enhancement via quasibound states to be dominant for other pairs of noble-gas and optically excited alkali atoms. Quasibound states originate from wells and barriers in the shape of the PEC, which appear in various alkali-noble-gas pairs [53,74,75] and are correlated with the shape of the electron density as shown for LiHe in Ref. [76]. For most resonant collisions, the interaction time is saturated by γ^{-1} , and therefore each resonance contributes similarly to $k_{se}^{(q)}$. The enhancement is thus proportional to the total number of resonances N_{res} , which predominantly depends on μ . By scaling μ in Eq. (1) for the K-³He potential, we find that $N_{\text{res}} \propto \mu$ as presented in Fig. 4(a). We verify this estimate by solving the scattering of electronically excited K-³⁷Ar pairs, using an *ab initio* 5S potential [77]. In Fig. 4(b) we show the increase in the number of resonances for K-³⁷Ar as expressed in the mean time delay. We characterize the enhancement by the resonances over binary polarization

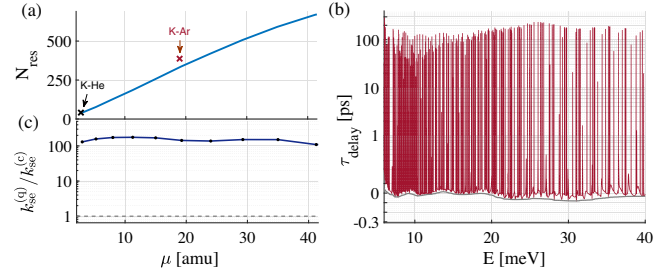


FIG. 4. Resonant spin-polarization transfer for different electronically excited alkali-noble-gas pairs. (a) The number of tunneling resonances N_{res} (blue line) increases linearly with μ , derived by solving the K-³He scattering in Eq. (1) scaled by μ . Crosses mark calculations for unscaled K-³He (black) and the true 5S PEC of K-³⁷Ar (brown). (b) Scattering time delay, for the heavier K-³⁷Ar pair. The number of resonances is dramatically increased compared with Fig. 3(d). (c) The enhancement in the polarization rate coefficient $k_{se}^{(q)}/k_{se}^{(c)}$ for the 5S potential by formation of tunneling resonances over binary collisions, which we estimate to be constant and independent of μ and α .

rate in Fig. 4(c) using the ratio $k_{se}^{(q)}/k_{se}^{(c)}$, which weakly depends on $\alpha(R)$ and on the specific colliding pair.

Resonant spin-exchange optical pumping of noble gas can be realized with various alkali and noble-gas mixtures, within a large range of experimental parameters. Here we present an exemplary configuration using a mixture of K-³He in a chip-scale cubic cell of length 2 mm and 3 Torr of helium. The resonant polarization transfer relies on optical pumping of potassium spins in the 5S state followed by random collisions with helium gas. The 5S state can efficiently be excited via a two-photon ladder scheme $4S \rightarrow 4P_{3/2} \rightarrow 5S$ using 766 nm and 1.25 μm light for the first and second transitions, respectively. The 4P level is pressure broadened, with homogeneous optical linewidth of about $\Gamma \approx 50$ MHz [31] and inhomogeneous Doppler broadening of 1 GHz. The dominant decay rate of the 5S state, $\gamma_0 = 3.8$ MHz, is radiative, as the coupling of S shells to orbital angular momentum is weak, suppressing destruction by spin rotation during collisions.

500 mW for each beam covering the cell yields Rabi frequencies exceeding 300 and 100 MHz. A 3 GHz one-photon detuning of the beams renders the transition $4S \rightarrow 5S$ through the P level virtual, suppressing spin relaxation by collisions in the P state, yielding a Raman rate $\Omega_R > 10$ MHz. Pulsed operation potentially enables near unity population as $p_{5S} \approx \Omega_R^2 / (\Omega_R^2 + \gamma_0^2/2)$ and about half that value for cw operation. The spin state of the 5S can be defined via controlling the polarizations of the beams and pumping of the 4S spin. For example, setting 766 nm light polarization circular, pumps the 4S spin and overcomes its 100 kHz depolarization rate by collisions with the walls, whereas the 1.25 μm light can be linearly polarized. If necessary, additional on-resonance pulses can maintain the

4S spin polarization and enable well-defined excitation channels. For the low-pressure configuration, the stringent estimation of $\gamma^{-1} = 1$ ns corresponds to a 100-fold enhancement of the polarization rate coefficient via resonant collisions [cf. Fig. 3(c)].

In summary, we analyzed the spin-polarization transfer in collisions of optically excited alkali and noble-gas atoms, using *ab initio* calculations of K-He and K-Ar pairs. We revealed the formation of quasibound states, manifested as sharp resonances in the scattering time delay and spin-exchange cross section. The resonances are expected to enhance the polarization transfer rate of noble gases by 2 orders of magnitude for a thermal ensemble at ambient conditions and up to 6 orders of magnitude at the resonance energies and be significant for different optically excited alkali and noble-gas pairs.

Various applications using spin-polarized gases can benefit from optically controlled enhancement of the polarization rate. Here we consider several potential avenues. Precision NMR sensors and comagnetometers use mixtures of noble-gas and alkali spins. The former sense external fields; the latter serve as an embedded optical magnetometer [78–83]. In miniaturized sensors, with significant alkali polarization loss to cell walls, initialization time and sensitivity can greatly benefit from enhanced polarization rates for all noble gases. This is much like the case of xenon, which can be quickly polarized and thus suitable for miniaturization [84]. Notably, the proposed mechanism is optically controlled, enhancing the polarization rate on demand within the standard operation of these sensors.

Magnetic resonance imaging of human air spaces with record resolution and preparation of neutron spin filters and targets use large volumes of polarized gas at atmospheric pressure or above. The method of metastability-exchange optical pumping (MEOP) enables rapid polarization of helium nuclei at low gas pressures. Subsequent compression then brings the polarized gas to a higher target pressure [10]. Whereas MEOP is exclusively limited to helium, the proposed technique enables quick low-pressure polarization of other noble-gas atoms, which may be more available or more appropriate for specific applications.

Several quantum information applications, such as optical quantum memories [19,20], generation of spin entanglement [18,85,86], and nonclassical coupling to optomechanical systems, like gravitational-wave detectors [87–89], can significantly benefit from the long spin lifetime of noble gases. These applications require a bidirectional interface between spins and light, overcoming classical noise to reach the standard quantum limit [90,91]. An efficient interface requires several ingredients, including high spin polarization, increased number densities, and strong optical interaction. The classical limiting noise typically scales with the number of noble-gas atoms in the cell. Therefore, quantum applications are likely to be

first realized at low pressures and at small volumes, conditions under which the proposed mechanism is most beneficial.

Finally, the resonant enhancement at particular kinetic energies is several orders of magnitude greater than the thermally averaged one. Cryogenic operation and use of velocity selective atomic beams might exploit that enhancement even further.

We thank Or Peleg, Roy Shaham, Yoav Sagi, and Edvardas Narevicius for fruitful discussions. We also thank Zohar Amitay for making available their results for the potassium-argon PEC. This research was supported by the Israel Science Foundation (Grant No. 1661/19).

*Present address: Department of Electrical and Computer Engineering, Duke University, Durham, North Carolina 27708, USA.

or.katz@duke.edu

- [1] T. W. Kornack, R. K. Ghosh, and M. V. Romalis, Nuclear Spin Gyroscope Based on an Atomic Comagnetometer, *Phys. Rev. Lett.* **95**, 230801 (2005).
- [2] T. G. Walker and M. S. Larsen, Spin-exchange-pumped NMR gyros, in *Advances in Atomic, Molecular, and Optical Physics* (Elsevier, New York, 2016), Vol. 65, pp. 373–401, 10.1016/bs.aamop.2016.04.002.
- [3] I. Kominis, T. Kornack, J. Allred, and M. Romalis, A subfemtotesla multichannel atomic magnetometer, *Nature (London)* **422**, 596 (2003).
- [4] A. O. Sushkov and D. Budker, Production of long-lived atomic vapor inside high-density buffer gas, *Phys. Rev. A* **77**, 042707 (2008).
- [5] M. Albert, G. Cates, B. Driehuys, W. Happer, B. Saam, C. Springer Jr, and A. Wishnia, Biological magnetic resonance imaging using laser-polarized ^{129}Xe , *Nature (London)* **370**, 199 (1994).
- [6] S. Fain, M. L. Schiebler, D. G. McCormack, and G. Parraga, Imaging of lung function using hyperpolarized helium-3 magnetic resonance imaging: Review of current and emerging translational methods and applications, *J. Magn. Reson. Imaging* **32**, 1398 (2010).
- [7] L. Flors, J. P. Mugler, A. Paget-Brown, D. K. Froh, E. E. de Lange, J. T. Patrie, and T. A. Altes, Hyperpolarized helium-3 diffusion-weighted magnetic resonance imaging detects abnormalities of lung structure in children with bronchopulmonary dysplasia, *Journal of thoracic imaging* **32**, 323 (2017).
- [8] P. Nikolaou, B. Goodson, and E. Chekmenev, NMR hyperpolarization techniques for biomedicine, *Chemistry* **21**, 3156 (2015).
- [9] M. J. Couch, B. Blasiak, B. Tomanek, A. V. Ouriadov, M. S. Fox, K. M. Dowhos, and M. S. Albert, Hyperpolarized and inert gas MRI: The future, *Mol. Imaging Biol.* **17**, 149 (2015).
- [10] T. R. Gentile, P. J. Nacher, B. Saam, and T. G. Walker, Optically polarized ^3He , *Rev. Mod. Phys.* **89**, 045004 (2017).

- [11] T.R. Gentile *et al.*, Polarized ^3He spin filters in neutron scattering, *Physica (Amsterdam)* **356B**, 96 (2005).
- [12] V.V. Flambaum, D. Budker, and A. Wickenbrock, Oscillating nuclear electric dipole moments inside atoms, [arXiv:1909.04970](https://arxiv.org/abs/1909.04970).
- [13] I.M. Bloch, Y. Hochberg, E. Kuflik, and T. Volansky, Axion-like relics: New constraints from old comagnetometer data, *J. High Energy Phys.* **01** (2020) 167.
- [14] J. Lee, A. Almasi, and M. V. Romalis, Improved Limits on Spin-Mass Interactions, *Phys. Rev. Lett.* **120**, 161801 (2018).
- [15] I.M. Bloch, G. Ronen, R. Shaham, O. Katz, T. Volansky, and O. Katz, Nasduck: New constraints on axion-like dark matter from Floquet quantum detector, [arXiv:2105.04603](https://arxiv.org/abs/2105.04603).
- [16] P.L. Anthony *et al.*, Determination of the Neutron Spin Structure Function, *Phys. Rev. Lett.* **71**, 959 (1993).
- [17] O. Katz, R. Shaham, and O. Firstenberg, Quantum interface for noble-gas spins, [arXiv:1905.12532](https://arxiv.org/abs/1905.12532) [PRX Quantum (to be published)].
- [18] O. Katz, R. Shaham, E. S. Polzik, and O. Firstenberg, Long-Lived Entanglement Generation of Nuclear Spins Using Coherent Light, *Phys. Rev. Lett.* **124**, 043602 (2020).
- [19] O. Katz, E. Reches, R. Shaham, A. V. Gorshkov, and O. Firstenberg, Optical quantum memory with optically inaccessible noble-gas spins, [arXiv:2007.08770](https://arxiv.org/abs/2007.08770).
- [20] A. Dantan, G. Reinaudi, A. Sinatra, F. Laloë, E. Giacobino, and M. Pinard, Long-Lived Quantum Memory with Nuclear Atomic Spins, *Phys. Rev. Lett.* **95**, 123002 (2005).
- [21] F. Colegrove, L. Scheerer, and G. Walters, Polarization of ^3He gas by optical pumping, *Phys. Rev.* **132**, 2561 (1963).
- [22] M. Batz, P.-J. Nacher, and G. Tostevin, Fundamentals of metastability exchange optical pumping in helium, *J. Phys. Conf. Ser.* **294**, 012002 (2011).
- [23] E. Stoltz, M. Meyerhoff, N. Bigelow, M. Leduc, P.-J. Nacher, and G. Tostevin, High nuclear polarization in ^3He and ^4He gas mixtures by optical pumping with a laser diode, *Appl. Phys. B* **63**, 629 (1996).
- [24] A. Nikiel-Osuchowska, G. Collier, B. Głowacz, T. Pałasz, Z. Olejniczak, W. P. Węglarz, G. Tostevin, P.-J. Nacher, and T. Dohnalik, Metastability exchange optical pumping of ^3He gas up to hundreds of millibars at 4.7 tesla, *Eur. Phys. J. D* **67**, 200 (2013).
- [25] T. Xia, S. W. Morgan, Y. Y. Jau, and W. Happer, Polarization and hyperfine transitions of metastable ^{129}Xe in discharge cells, *Phys. Rev. A* **81**, 033419 (2010).
- [26] V. Lefevre-Seguin and M. Leduc, Metastability-exchange and depolarising collisions in xenon and krypton, *J. Phys. B* **10**, 2157 (1977).
- [27] T. Hadeishi and C.-H. Liu, Observation of Spin Exchange between the Singly Ionized Xe^+ Ground State and the Metastable State of Neutral Xenon, *Phys. Rev. Lett.* **17**, 513 (1966).
- [28] A. Kastler, Some suggestions concerning the production and detection by optical means of inequalities in the populations of levels of spatial quantization in atoms. Application to the Stern and Gerlach and magnetic resonance experiments, *J. Phys. Radium* **11**, 255 (1950).
- [29] J. Brossel, A. Kastler, and J. Winter, Création optique d'une inégalité de population entre les sous-niveaux Zeeman de l'état fondamental des atomes, *J. Phys. Radium* **13**, 668 (1952).
- [30] W. Happer, Optical pumping, *Rev. Mod. Phys.* **44**, 169 (1972).
- [31] W. Happer, Y.-Y. Jau, and T.G. Walker, *Optically Pumped Atoms* (John Wiley & Sons, New York, 2010), <https://www.wiley.com/en/Optically+Pumped+Atoms-p-9783527407071>.
- [32] T. G. Walker and W. Happer, Spin-exchange optical pumping of noble-gas nuclei, *Rev. Mod. Phys.* **69**, 629 (1997).
- [33] H. M. J. M. Boesten, C. C. Tsai, J. R. Gardner, D. J. Heinzen, and B. J. Verhaar, Observation of a shape resonance in the collision of two cold Rb 87 atoms, *Phys. Rev. A* **55**, 636 (1997).
- [34] C. Chin, R. Grimm, P. Julienne, and E. Tiesinga, Feshbach resonances in ultracold gases, *Rev. Mod. Phys.* **82**, 1225 (2010).
- [35] S. Dürr, T. Volz, N. Syassen, G. Rempe, E. van Kempen, S. Kokkelmans, B. Verhaar, and H. Friedrich, Dissociation of Feshbach molecules into different partial waves, *Phys. Rev. A* **72**, 052707 (2005).
- [36] I. Bloch, J. Dalibard, and W. Zwerger, Many-body physics with ultracold gases, *Rev. Mod. Phys.* **80**, 885 (2008).
- [37] T. Sikorsky, M. Morita, Z. Meir, A. A. Buchachenko, R. Ben-shlomi, N. Akerman, E. Narevicius, T. V. Tscherbul, and R. Ozeri, Phase Locking between Different Partial Waves in Atom-Ion Spin-Exchange Collisions, *Phys. Rev. Lett.* **121**, 173402 (2018).
- [38] A. Klein, Y. Shagam, W. Skomorowski, P. S. Żuchowski, M. Pawlak, L. M. Janssen, N. Moiseyev, S. Y. van de Meerakker, A. van der Avoird, C. P. Koch *et al.*, Directly probing anisotropy in atom-molecule collisions through quantum scattering resonances, *Nat. Phys.* **13**, 35 (2017).
- [39] M. Tomza, K. Jachymski, R. Gerritsma, A. Negretti, T. Calarco, Z. Idziaszek, and P. S. Julienne, Cold hybrid ion-atom systems, *Rev. Mod. Phys.* **91**, 035001 (2019).
- [40] M. Tomza, C. P. Koch, and R. Moszynski, Cold interactions between an Yb^+ ion and a Li atom: Prospects for sympathetic cooling, radiative association, and Feshbach resonances, *Phys. Rev. A* **91**, 042706 (2015).
- [41] A. B. Henson, S. Gersten, Y. Shagam, J. Narevicius, and E. Narevicius, Observation of resonances in Penning ionization reactions at sub-kelvin temperatures in merged beams, *Science* **338**, 234 (2012).
- [42] S. Chefdeville, Y. Kalugina, S. Y. van de Meerakker, C. Naulin, F. Lique, and M. Costes, Observation of partial wave resonances in low-energy $\text{O}_2\text{--H}_2$ inelastic collisions, *Science* **341**, 1094 (2013).
- [43] N. R. Thomas, N. Kjærgaard, P. S. Julienne, and A. C. Wilson, Imaging of s and d Partial-Wave Interference in Quantum Scattering of Identical Bosonic Atoms, *Phys. Rev. Lett.* **93**, 173201 (2004).
- [44] T. G. Walker and W. Happer, Spin-rotation interaction of noble-gas alkali-metal atom pairs, *Rev. Mod. Phys.* **44**, 169 (1972).
- [45] N. Moiseyev, *Non-Hermitian Quantum Mechanics* (Cambridge University Press, Cambridge, England, 2011), [10.1017/CBO9780511976186](https://doi.org/10.1017/CBO9780511976186).
- [46] J. J. Sakurai and J. Napolitano, *Modern Quantum Mechanics*, 2nd ed. (Cambridge University Press, Cambridge, England, 2017), [10.1017/9781108499996](https://doi.org/10.1017/9781108499996).

- [47] G. Schultz, Resonances in electron impact on atoms, *Rev. Mod. Phys.* **45**, 378 (1973).
- [48] R. N. Zare, Resonances in reaction dynamics, *Science* **311**, 1383 (2006).
- [49] S. Hirata, M. Nooijen, and R. J. Bartlett, High-order determinantal equation-of-motion coupled-cluster calculations for ionized and electron-attached states, *Chem. Phys. Lett.* **328**, 459 (2000).
- [50] A. I. Krylov, Equation-of-motion coupled-cluster methods for open-shell and electronically excited species: The hitchhiker's guide to Fock space, *Annu. Rev. Phys. Chem.* **59**, 433 (2008).
- [51] Y. Shao, Z. Gan, E. Epifanovsky, A. T. Gilbert, M. Wormit, J. Kussmann, A. W. Lange, A. Behn, J. Deng, X. Feng *et al.*, Advances in molecular quantum chemistry contained in the Q-Chem 4 program package, *Mol. Phys.* **113**, 184 (2015).
- [52] M. Bucher, The electron inside the nucleus: An almost classical derivation of the isotropic hyperfine interaction, *Eur. J. Phys.* **21**, 19 (2000).
- [53] L. Blank, D. E. Weeks, and G. S. Kedziora, M + Ng potential energy curves including spin-orbit coupling for M = K, Rb, Cs and Ng = He, Ne, Ar, *J. Chem. Phys.* **136**, 124315 (2012).
- [54] See Supplemental Material at <http://link.aps.org/supplemental/10.1103/PhysRevLett.128.013401>, which includes (1) technical details of ab initio calculation for the K-³He complex, (2) potential energy curves and values of the hyperfine coupling constant, and (3) validation of calculation results by comparison with experiment, which includes Refs. [55–66].
- [55] H. Partridge, J. R. Stallcop, and E. Levin, Potential energy curves and transport properties for the interaction of He with other ground-state atoms, *J. Chem. Phys.* **115**, 6471 (2001).
- [56] F. Jensen, Polarization consistent basis sets. VII. The elements K, Ca, Ga, Ge, As, Se, Br, and Kr, *J. Chem. Phys.* **136**, 114107 (2012).
- [57] K. L. Schuchardt, B. T. Didier, T. Elsethagen, L. Sun, V. Gurumoorthi, J. Chase, J. Li, and T. L. Windus, Basis set exchange: A community database for computational sciences, *J. Chem. Inf. Model.* **47**, 1045 (2007).
- [58] E. Davidson, *Reduced Density Matrices in Quantum Chemistry* (Elsevier, New York, 2012), Vol. 6, <https://www.sciencedirect.com/bookseries/theoretical-chemistry/vol/6/suppl/C>.
- [59] W. Kutzelnigg, Origin and meaning of the Fermi contact interaction, *Theor. Chim. Acta* **73**, 173 (1988).
- [60] S. R. Schaefer, G. D. Cates, T.-R. Chien, D. Gonatas, W. Happer, and T. G. Walker, Frequency shifts of the magnetic-resonance spectrum of mixtures of nuclear spin-polarized noble gases and vapors of spin-polarized alkali-metal atoms, *Phys. Rev. A* **39**, 5613 (1989).
- [61] E. Babcock, I. A. Nelson, S. Kadlecsek, and T. G. Walker, ³He polarization-dependent EPR frequency shifts of alkali-metal—³He pairs, *Phys. Rev. A* **71**, 013414 (2005).
- [62] E. Babcock, I. Nelson, S. Kadlecsek, B. Driehuys, L. W. Anderson, F. W. Hersman, and T. G. Walker, Hybrid Spin-Exchange Optical Pumping of ³He, *Phys. Rev. Lett.* **91**, 123003 (2003).
- [63] E. D. Babcock, Spin-exchange optical pumping with alkali-metal vapors, Ph.D. thesis, University of Wisconsin-Madison, 2005, <https://pages.physics.wisc.edu/~tgwalker/Theses/2005Babcock.pdf>.
- [64] T. G. Walker, I. A. Nelson, and S. Kadlecsek, Method for deducing anisotropic spin-exchange rates, *Phys. Rev. A* **81**, 032709 (2010).
- [65] J. T. Singh, P. A. M. Dolph, W. A. Tobias, T. D. Averett, A. Kelleher, K. E. Mooney, V. V. Nelyubin, Y. Wang, Y. Zheng, and G. D. Cates, Development of high-performance alkali-hybrid polarized ³He targets for electron scattering, *Phys. Rev. C* **91**, 055205 (2015).
- [66] K. Boguslawski, K. H. Marti, Ö. Legeza, and M. Reiher, Accurate ab initio spin densities, *J. Chem. Theory Comput.* **8**, 1970 (2012).
- [67] P. A. Batishchev and O. I. Tolstikhin, Siegert pseudostate formulation of scattering theory: Nonzero angular momenta in the one-channel case, *Phys. Rev. A* **75**, 062704 (2007).
- [68] O. I. Tolstikhin, V. N. Ostrovsky, and H. Nakamura, Siegert pseudostate formulation of scattering theory: One-channel case, *Phys. Rev. A* **58**, 2077 (1998).
- [69] W. Happer, E. Miron, S. Schaefer, D. Schreiber, W. A. van Wijngaarden, and X. Zeng, Polarization of the nuclear spins of noble-gas atoms by spin exchange with optically pumped alkali-metal atoms, *Phys. Rev. A* **29**, 3092 (1984).
- [70] T. G. Walker, Estimates of spin-exchange parameters for alkali-metal–noble-gas pairs, *Phys. Rev. A* **40**, 4959 (1989).
- [71] D. J. Griffiths and D. F. Schroeter, *Introduction to Quantum Mechanics* (Cambridge University Press, Cambridge, England, 2018), <https://www.cambridge.org/en/academic/subjects/physics/quantum-physics-quantum-information-and-quantum-computation/introduction-quantum-mechanics-3rd-edition>.
- [72] A. Chattopadhyay, A comparative spectroscopic study of the excited electronic states of potassium-neon and potassium-helium systems, *Eur. Phys. J. D* **66**, 325 (2012).
- [73] S. Kontar and M. Korek, Electronic structure with a dipole moment calculation of the low-lying electronic states of the KHe molecule, *J. Struct. Chem.* **58**, 23 (2017).
- [74] F. Masnou-Seeuws, Model potential calculations for the KHe and KNe molecular systems: comparison with the predictions of the asymptotic methods, *J. Phys. B* **15**, 883 (1982).
- [75] A. Tam, G. Moe, W. Park, and W. Happer, Strong New Emission Bands in Alkali-Noble-Gas Systems, *Phys. Rev. Lett.* **35**, 85 (1975).
- [76] A. Yiannopoulou, G.-H. Jeung, S. J. Park, H. S. Lee, and Y. S. Lee, Undulations of the potential-energy curves for highly excited electronic states in diatomic molecules related to the atomic orbital undulations, *Phys. Rev. A* **59**, 1178 (1999).
- [77] Z. Amitay (private communication).
- [78] D. Bevan, M. Bulatowicz, P. Clark, R. Griffith, M. Larsen, M. Luengo-Kovac, and J. Pavell, Compact atomic magnetometer for global navigation (nav-cam), in *Proceedings of the 2018 IEEE International Symposium on Inertial Sensors and Systems (INERTIAL)* (IEEE, New York, 2018), pp. 1–2, 10.1109/ISISS.2018.8358161.

- [79] J. Fang, J. Qin, S. Wan, Y. Chen, and R. Li, Atomic spin gyroscope based on ^{129}Xe -Cs comagnetometer, *Chin. Sci. Bull.* **58**, 1512 (2013).
- [80] T. Walker and M. Larsen, Chapter eight—spin-exchange-pumped NMR gyros, *Adv. At. Mol. Opt. Phys.* **65**, 373 (2016).
- [81] M. E. Limes, D. Sheng, and M. V. Romalis, ^3He — ^{129}Xe Comagnetometry using ^{87}Rb Detection and Decoupling, *Phys. Rev. Lett.* **120**, 033401 (2018).
- [82] E. Zeuthen, E. S. Polzik, and F. Y. Khalili, Gravitational wave detection beyond the standard quantum limit using a negative-mass spin system and virtual rigidity, *Phys. Rev. D* **100**, 062004 (2019).
- [83] F. Y. Khalili and E. S. Polzik, Overcoming the Standard Quantum Limit in Gravitational Wave Detectors Using Spin Systems with a Negative Effective Mass, *Phys. Rev. Lett.* **121**, 031101 (2018).
- [84] R. Jiménez-Martínez, D. J. Kennedy, M. Rosenbluh, E. A. Donley, S. Knappe, S. J. Seltzer, H. L. Ring, V. S. Bajaj, and J. Kitching, Optical hyperpolarization and NMR detection of ^{129}Xe on a microfluidic chip, *Nat. Commun.* **5**, 3908 (2014).
- [85] G. Reinaudi, A. Sinatra, A. Dantan, and M. Pinard, Squeezing and entangling nuclear spins in helium 3, *J. Mod. Opt.* **54**, 675 (2007).
- [86] A. Serafin, M. Fadel, P. Treutlein, and A. Sinatra, Nuclear Spin Squeezing in Helium-3 by Continuous Quantum Nondemolition Measurement, *Phys. Rev. Lett.* **127**, 013601 (2021).
- [87] C. B. Møller, R. A. Thomas, G. Vasilakis, E. Zeuthen, Y. Tsaturyan, M. Balabas, K. Jensen, A. Schliesser, K. Hammerer, and E. S. Polzik, Quantum back-action-evading measurement of motion in a negative mass reference frame, *Nature (London)* **547**, 191 (2017).
- [88] R. A. Thomas, M. Parniak, C. Østfeldt, C. B. Møller, C. Bærentsen, Y. Tsaturyan, A. Schliesser, J. Appel, E. Zeuthen, and E. S. Polzik, Entanglement between distant macroscopic mechanical and spin systems, *Nat. Phys.* **17**, 228 (2021).
- [89] F. Y. Khalili and E. S. Polzik, Overcoming the Standard Quantum Limit in Gravitational Wave Detectors using Spin Systems with a Negative Effective Mass, *Phys. Rev. Lett.* **121**, 031101 (2018).
- [90] R. Shaham, O. Katz, and O. Firstenberg, Strong coupling of alkali spins to noble-gas spins with hour-long coherence time, *arXiv:2102.02797*.
- [91] O. Katz, R. Shaham, and O. Firstenberg, Coupling light to a nuclear spin gas with a two-photon linewidth of five millihertz, *Sci. Adv.* **7**, eabe9164 (2021).